

Tests of lepton flavour universality using semitauonic B decays at LHCb

Adam Morris, on behalf of the LHCb collaboration

Aix Marseille Univ, CNRS/IN2P3, CPPM

10th International Workshop on the CKM Unitarity Triangle
Heidelberg, 20th September, 2018



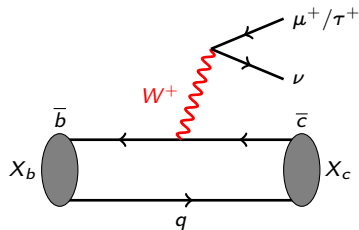
Lepton Flavour Universality (LFU):

- In SM, electroweak couplings of charged leptons are identical (universal).
- Difference between e , μ and τ should therefore only be driven by mass.
- Test: **ratios of branching fractions** to final states differing by lepton flavour.

LFU tests in semitauonic b -hadron decays:

$$R(X_c) = \frac{\mathcal{B}(X_b \rightarrow X_c \tau^+ \nu_\tau)}{\mathcal{B}(X_b \rightarrow X_c \mu^+ \nu_\mu)}$$

(X_b : b -hadron, X_c : c -hadron)



Introduction

In this talk:

- $R(D^*)$ hadronic: $B^0 \rightarrow D^{*-} \ell^+ \nu$ with $\tau^+ \rightarrow 3\pi^\pm (\pi^0) \bar{\nu}_\tau$.
- $R(D^*)$ muonic: $B^0 \rightarrow D^{*-} \ell^+ \nu$ with $\tau^+ \rightarrow \mu^+ \nu_\mu \bar{\nu}_\tau$.
- $R(J/\psi)$ muonic: $B_c^+ \rightarrow J/\psi \ell^+ \nu$ with $\tau^+ \rightarrow \mu^+ \nu_\mu \bar{\nu}_\tau$.
- Complementary strategies: different backgrounds and systematics.
- LHCb 2011+2012 data: 3 fb^{-1} at $\sqrt{s} = 7\&8 \text{ TeV}$.
- Using $D^{*-} \rightarrow \bar{D}^0 (\rightarrow K^+ \pi^-) \pi^-$ and $J/\psi \rightarrow \mu^+ \mu^-$.

Mode	BF (%)
$\tau^- \rightarrow \pi^- \pi^0 \nu_\tau$	25.49 ± 0.09
$\tau^- \rightarrow e^- \bar{\nu}_e \nu_\tau$	17.82 ± 0.04
$\tau^- \rightarrow \mu^- \bar{\nu}_\mu \nu_\tau$	17.39 ± 0.04
$\tau^- \rightarrow \pi^- \nu_\tau$	10.82 ± 0.05
$\tau^- \rightarrow 3\pi^\mp \nu_\tau$	9.31 ± 0.05
$\tau^- \rightarrow 3\pi^\mp \pi^0 \nu_\tau$	4.62 ± 0.05

[PDG]

Predictions:

- $R(D^*) = 0.258 \pm 0.005$ [HFLAV Summer 2018]
- $R(J/\psi) \in [0.25, 0.28]$ [PLB452 (1999) 120, arXiv:0211021, PRD73 (2006) 054024, PRD74 (2006) 074008]

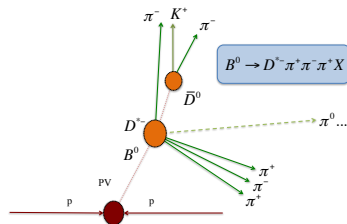
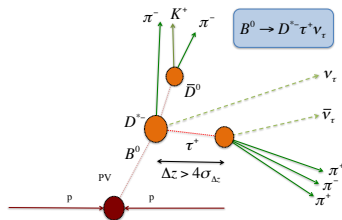
$$R(D^*) \text{ with } \tau^+ \rightarrow 3\pi^\pm(\pi^0)\bar{\nu}_\tau$$

$R(D^*)$ hadronic: introduction

$$\mathcal{K}(D^*) = \frac{\mathcal{B}(B^0 \rightarrow D^{*-} \tau^+ \nu_\tau)}{\mathcal{B}(B^0 \rightarrow D^{*-} 3\pi^\pm)} = \frac{N_{\text{sig}} \epsilon_{\text{norm}}}{N_{\text{norm}} \epsilon_{\text{sig}}} \frac{1}{\mathcal{B}(\tau^+ \rightarrow 3\pi^\pm(\pi^0)\bar{\nu}_\tau)}$$

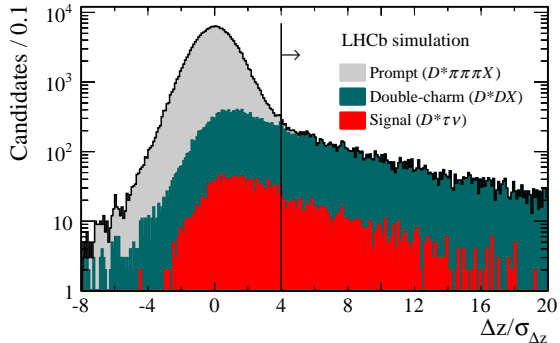
- Signal and normalisation **same visible final state: $D^{*-} 3\pi^\pm$** .
- N_{sig} from 3D binned template fit:
 - $q^2 \equiv |P_{B^0} - P_{D^*}|^2$,
 - τ^+ decay time,
 - Output of BDT trained to discriminate signal from $D^* D_s^+$.
- N_{norm} from unbinned max likelihood fit to $m(D^* 3\pi^\pm)$.
- Make use of **three-prong tau vertex** in selection.
- Convert $\mathcal{K}(D^*)$ to $R(D^*)$:

$$R(D^*) = \mathcal{K}(D^*) \frac{\mathcal{B}(B^0 \rightarrow D^{*-} 3\pi^\pm)}{\mathcal{B}(B^0 \rightarrow D^{*-} \mu^+ \nu_\mu)}$$



$R(D^*)$ hadronic: backgrounds

- Most abundant background: $X_b \rightarrow D^{*-} 3\pi^\pm X$.
 - $\sim 100\times$ more abundant than signal.
 - Suppressed by requiring τ^+ vertex to be $4\sigma_{\Delta z}$ downstream from B vertex.
 - Improves S/B by factor 160.
- Remaining backgrounds: **double charm modes with non-negligible lifetimes:**
 - $X_b \rightarrow D^* D_s^+ X \sim 10\times$ signal,
 - $X_b \rightarrow D^* D^+ X \sim 1\times$ signal,
 - $X_b \rightarrow D^* D^0 X \sim 0.2\times$ signal.

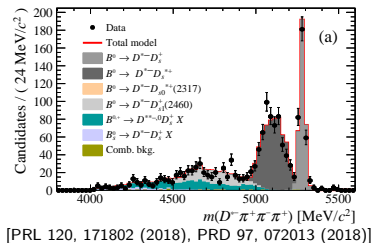
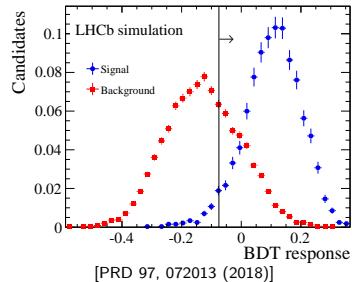


[PRD 97, 072013 (2018)]

$R(D^*)$ hadronic: backgrounds

Discriminate between signal and double charm backgrounds using a BDT that exploits the resonant structures in the $3\pi^\pm$ systems from τ^+ and D_s^+ decays.

Control samples of $D^*D_s^+X$, D^*D^+X and D^*D^0X used to correct simulation.



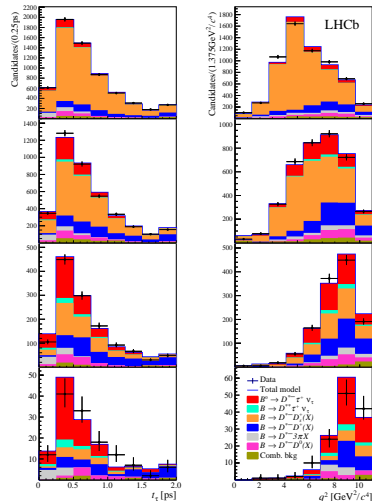
$R(D^*)$ hadronic: fit and result

- Projections of 3D binned template fit shown for $t(\tau)$ (left) and q^2 (right) for each of the BDT bins.
- **Signal** purity increases with BDT output, while $D^*D_s^+X$ fraction decreases.
- Dominant background at high BDT output D^*D^+X due to long D^+ lifetime.
- $N_{\text{sig}} = 1296 \pm 86$, $N_{\text{norm}} = 17660 \pm 158$.

$$\mathcal{K}(D^*) = 1.97 \pm 0.13 (\text{stat}) \pm 0.18 (\text{syst})$$

$$R(D^*) = 0.291 \pm 0.019 (\text{stat}) \pm 0.026 (\text{syst}) \pm 0.013 (\text{ext}).$$

- 0.9σ above SM, compatible with experimental average.



[PRL 120, 171802 (2018), PRD 97, 072013 (2018)]

$R(D^*)$ hadronic: systematic uncertainties

- Largest systematic uncertainty is **MC statistics**.
- Uncertainties on double charm backgrounds should improve with **more data** and **improved external measurements**.
- Uncertainty on efficiency ratio should improve with more statistics.

Source	$\frac{\delta R(D^*)}{R(D^*)}$ [%]
Simulated sample size	4.7
Empty bins in templates	1.3
Signal decay model	1.8
$D^{**}\tau\nu_\tau$ and $D_s^{**}\tau\nu_\tau$ feed-down	2.7
$D_s^+ \rightarrow 3\pi^\pm X$ decay model	2.5
$B \rightarrow D^*D_s^+ X$, $D^*D^+ X$, $D^*D^0 X$ backgrounds	3.9
Combinatorial background	0.7
$B \rightarrow D^{*-}3\pi^\pm X$ background	2.8
Efficiency ratio	3.9
Normalisation channel efficiency (modelling of $B^0 \rightarrow D^{*-}3\pi^\pm$)	2.0
Total systematic uncertainty	9.1

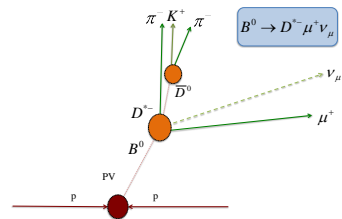
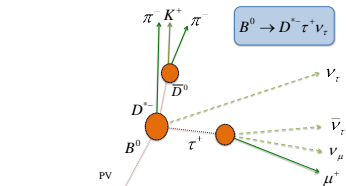
[PRL 120, 171802 (2018), PRD 97, 072013 (2018)]

$$R(D^*) \text{ with } \tau^+ \rightarrow \mu^+ \nu_\mu \bar{\nu}_\tau$$

$R(D^*)$ muonic: introduction

$$R(D^*) = \frac{\mathcal{B}(B^0 \rightarrow D^{*-} \tau^+ \nu_\tau)}{\mathcal{B}(B^0 \rightarrow D^{*-} \mu^+ \nu_\mu)}$$

- Both modes have **same visible final state: $D^{*-} \mu^+$** .
- Neither fully reconstructable, due to neutrinos.
 - B^0 momentum approximated using B^0 decay vertex and scaling visible longitudinal momentum by $m(B^0)/m(D^{*-} \mu^+)$
 - Resolution on kinematic variables enough to distinguish between τ/μ modes.
- 3D binned template fit to extract yields:
 - $q^2 \equiv |P_{B^0} - P_{D^*}|^2$,
 - $m_{\text{miss}}^2 \equiv |P_{B^0} - P_{D^*} - P_{\mu^+}|^2$,
 - $E_{\mu^+}^* \equiv$ muon energy in B^0 rest frame.

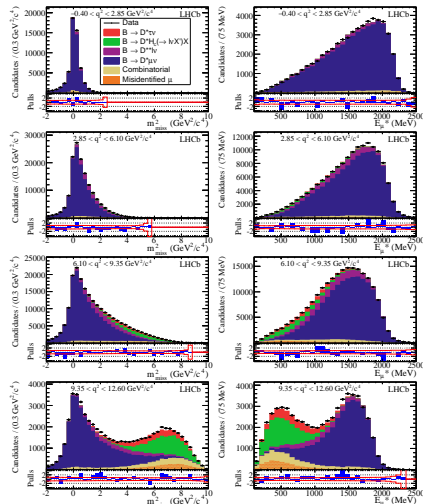


$R(D^*)$ muonic: fit and result

- Projections of 3D binned template fit shown for m_{miss}^2 (left) and $E_{\mu^+}^*$ (right) in each of the q^2 bins
- Dominant component is $B^0 \rightarrow D^* \mu^+ \nu_\mu$
- $B^0 \rightarrow D^* \tau^+ \nu_\tau$ signal purity increases with q^2
- Backgrounds:
 - D^{**} feed-down
 - Double charm
 - Combinatorial
 - Misidentified muon

$$R(D^*) = 0.336 \pm 0.027 \text{ (stat)} \pm 0.030 \text{ (syst)}$$

- 1.9σ above SM



[PRL 115, 112001 (2015)]

$R(D^*)$ muonic: systematics

- **MC statistics** largest systematic.
- Mis-ID μ template: reduce with **improved rejection** and more sophisticated technique.

Source	$\delta R(D^*) [\times 10^{-2}]$
Simulated sample size (model)	2.0
Misidentified μ template shape	1.6
$\bar{B}^0 \rightarrow D^{*+}(\tau^-/\mu^-)\bar{\nu}$ form factors	0.6
$\bar{B} \rightarrow D^{*+} X_c (\rightarrow \mu \nu X')$ shape corrections	0.5
$\mathcal{B}(\bar{B} \rightarrow D^{**} \tau^- \bar{\nu}_\tau) / \mathcal{B}(\bar{B} \rightarrow D^{**} \mu^- \nu_\mu)$	0.5
$\bar{B} \rightarrow D^{**} (\rightarrow D^* \pi \pi) \mu \nu$ shape corrections	0.4
Corrections to simulation	0.4
Combinatorial background shape	0.3
$\bar{B} \rightarrow D^{**} (\rightarrow D^{*+} \pi) \mu^- \bar{\nu}_\mu$ form factors	0.3
$\bar{B} \rightarrow D^{*+} (D_s^+ \rightarrow \tau \nu) X$ fraction	0.1
Simulated sample size (normalisation)	0.6
Hardware trigger efficiency	0.6
Particle identification efficiencies	0.3
Form-factors	0.2
$\mathcal{B}(\tau^- \rightarrow \mu^- \bar{\nu}_\mu \nu_\tau)$	< 0.1
Total systematic uncertainty	3.0

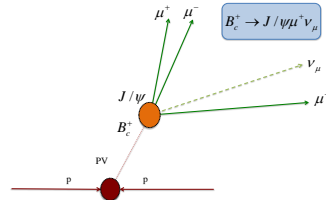
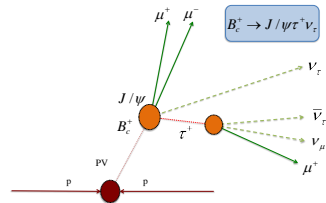
[PRL 115, 112001 (2015)]

$$R(J/\psi) \text{ with } \tau^+ \rightarrow \mu^+ \nu_\mu \bar{\nu}_\tau$$

R(J/ψ) muonic: introduction

$$R(J/\psi) = \frac{\mathcal{B}(B_c^+ \rightarrow J/\psi \tau^+ \nu_\tau)}{\mathcal{B}(B_c^+ \rightarrow J/\psi \mu^+ \nu_\mu)}$$

- Both modes have **same visible final state: $J/\psi \mu^+$** .
- 3D binned template fit to extract yields:
 - B_c^+ decay time,
 - m_{miss}^2 ,
 - $Z(E_{\mu^+}^*, q^2) \equiv$ flattened 4×2 histogram of $E_{\mu^+}^*$ and q^2 .
- B_c^+ decay form factors not precisely determined; constrained experimentally from this analysis.
- Low rate of B_c^+ production, but no long-lived D -meson background.

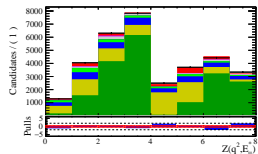
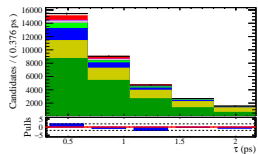
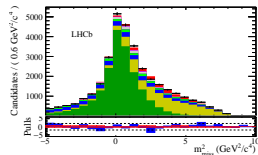


$R(J/\psi)$ muonic: fit and result

- Projections of 3D binned template fit shown.
- Largest component is $B_c^+ \rightarrow J/\psi \mu^+ \nu_\mu$ (19 140 \pm 340 candidates).
- $B_c^+ \rightarrow J/\psi \tau^+ \nu_\tau$ in red (1 400 \pm 300 candidates).
- Main background: $X_b \rightarrow J/\psi + \text{mis-ID hadron}$.
- **First evidence** of the decay $B_c^+ \rightarrow J/\psi \tau^+ \nu_\tau$ (3σ significance).

$$R(J/\psi) = 0.71 \pm 0.17 (\text{stat}) \pm 0.18 (\text{syst})$$

- 2σ above the SM.



[PRL 120, 121801 (2018)]

$R(J/\psi)$ muonic: systematics

- B_c^+ form factors: recent improvements should enter into updated measurement.
- MC statistics second-largest systematic.

Source	$\delta R(J/\psi) [\times 10^{-2}]$
Simulation sample size	8.0
$B_c^+ \rightarrow J/\psi$ form factors	12.1
$B_c^+ \rightarrow \psi(2S)$ form factors	3.2
Bias correction	5.4
$B_c^+ \rightarrow J/\psi X_c X$ cocktail composition	3.6
Z binning strategy	5.6
Misidentification background strategy	5.4
Combinatorial background cocktail	4.5
Combinatorial J/ψ sideband scaling	0.9
Empirical reweighting	1.6
Semitauponic $\psi(2S)$ and χ_c feed-down	0.9
Fixing $A_2(q^2)$ slope to zero	0.3
Efficiency ratio	0.6
$\mathcal{B}(\tau^+ \rightarrow \mu^+ \nu_\mu \bar{\nu}_\tau)$	0.2
Total systematic uncertainty	17.7

[PRL 120, 121801 (2018)]

Summary and conclusions

Summary

LHCb has made 3 tests of LFU with semitauonic B decays so far:

$$R(D^*) \text{ (hadronic)} = 0.291 \pm 0.019 \text{ (stat)} \pm 0.026 \text{ (syst)} \pm 0.013 \text{ (ext)},$$

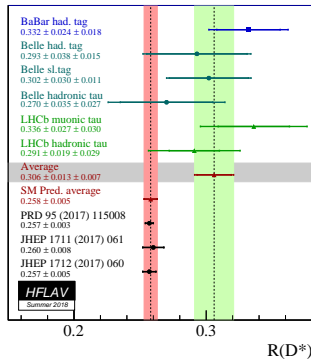
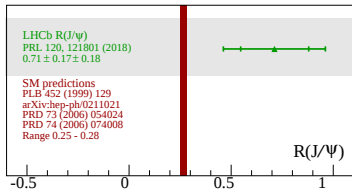
$$R(D^*) \text{ (muonic)} = 0.336 \pm 0.027 \text{ (stat)} \pm 0.030 \text{ (syst)},$$

$$R(J/\psi) = 0.71 \pm 0.17 \text{ (stat)} \pm 0.18 \text{ (syst)}.$$

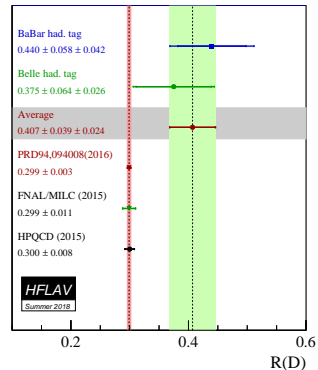
Average of LHCb $R(D^*)$ results is 1.9σ above SM:

$$R(D^*) = 0.310 \pm 0.016 \text{ (stat)} \pm 0.022 \text{ (syst)}.$$

World averages



[HFLAV Summer 2018]

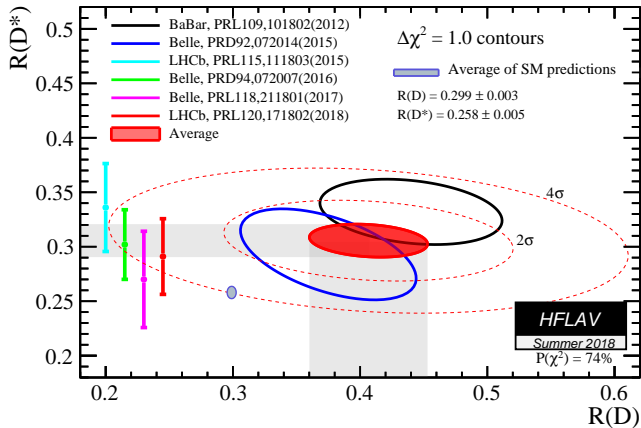
 $R(D)$ included for context

Between LHCb, BaBar and Belle: 9 measurements of LFU with semitauonic B decays so far.

- $6 \times R(D^*)$, $2 \times R(D)$, $1 \times R(J/\psi)$.
- All lie above the SM expectation.
- $R(D^*)$ average 3.0σ from SM.

World averages

- HFLAV summer 2018
 $R(D) - R(D^*)$ average is 3.8σ
from the SM.
- Reduction from 4.1σ due to
increase in theory uncertainties.



[HFLAV Summer 2018]

Conclusions and prospects

- **Hints of LFU violation** in semitauonic B decays.
 - $R(D) - R(D^*)$: 3.8σ away from SM.
 - $R(J/\psi)$: 2σ above SM.
- LHCb results only use Run 1 data: Runs 2,3,4... will bring much larger statistics.
- Many systematics will reduce with more data and more MC
- Others will reduce with improved external measurements (BESIII, Belle II)
- Analyses of more modes:
 - $b \rightarrow c\tau^-\bar{\nu}_\tau$: $R(D^+)$, $R(D^0)$, $R(D_s^{+(*)})$, $R(\Lambda_c^{+(*)})$...
 - $b \rightarrow u\tau^-\bar{\nu}_\tau$: $\Lambda_b^0 \rightarrow p\tau^-\bar{\nu}_\tau$, $B^+ \rightarrow p\bar{p}\tau^+\nu_\tau$...
- New observables beyond ratios of branching fractions, e.g. angular analyses to discriminate between NP models.

Backup slides

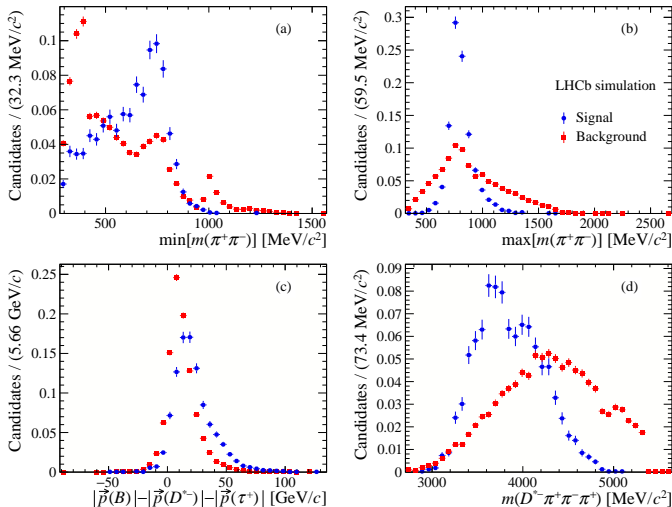
$$R(D^*) \text{ with } \tau^+ \rightarrow 3\pi^\pm(\pi^0)\bar{\nu}_\tau$$

$R(D^*)$ hadronic

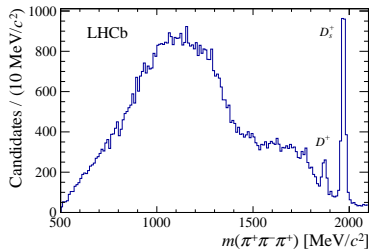
$$R(D^*) = \mathcal{K}(D^*) \frac{\mathcal{B}(B^0 \rightarrow D^{*-} 3\pi^\pm)}{\mathcal{B}(B^0 \rightarrow D^{*-} \mu^+ \nu_\mu)}$$

$$\mathcal{K}(D^*) = \frac{N_{\text{sig}}}{N_{\text{norm}}} \frac{\epsilon_{\text{norm}}}{\epsilon_{\text{sig}}} \frac{1}{\mathcal{B}(\tau^+ \rightarrow 3\pi^\pm(\pi^0)\bar{\nu}_\tau)}$$

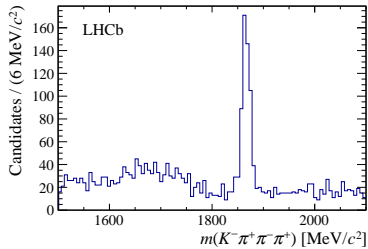
- N_{sig} from 3D binned template fit
- N_{norm} from unbinned fit to $m(D^{*-} 3\pi^\pm)$
- Efficiencies ϵ from MC
- $\mathcal{B}(\tau^+ \rightarrow 3\pi^\pm \bar{\nu}_\tau) = (9.31 \pm 0.05)\%$ [PDG]
- $\mathcal{B}(\tau^+ \rightarrow 3\pi^\pm \pi^0 \bar{\nu}_\tau) = (4.61 \pm 0.05)\%$ [PDG]
- $\mathcal{B}(B^0 \rightarrow D^{*-} 3\pi^\pm)$ [LHCb, BaBar, Belle]
- $\mathcal{B}(B^0 \rightarrow D^{*-} \mu^+ \nu_\mu)$ [PDG]

$R(D^*)$ hadronic: BDT

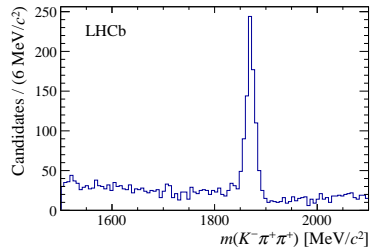
$R(D^*)$ hadronic: D_s^+ , D^0 , D^+ control channels



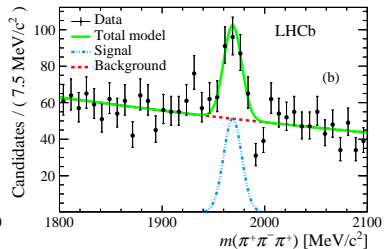
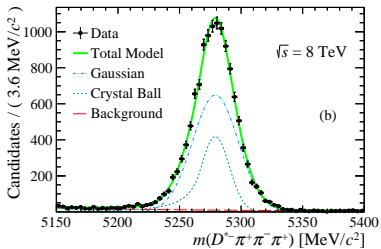
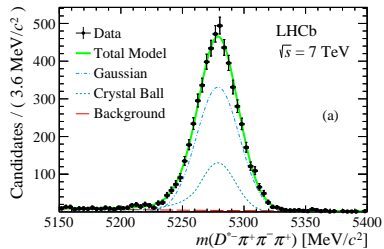
Distribution of $m(3\pi^\pm)$ for candidates passing the detached-vertex cut. The D^+ and D_s^+ peaks are visible.



Distribution of $m(K^- 3\pi^\pm)$ where a charged kaon has been associated to the $3\pi^\pm$ vertex (anti-isolation). The D^0 peak is visible.

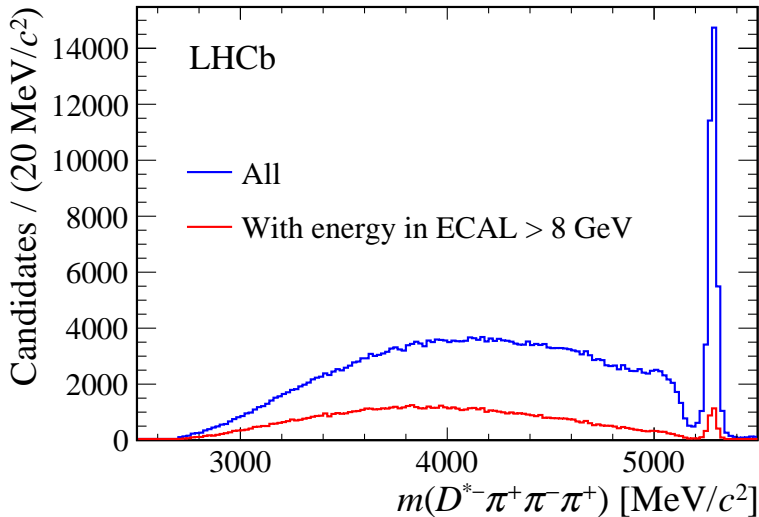


Distribution of $m(K^- \pi^+ \pi^+)$ for candidates passing the signal selection, where a π^- has been assigned the kaon mass (anti-PID). The D^+ peak is visible.

$R(D^*)$ hadronic: normalisation

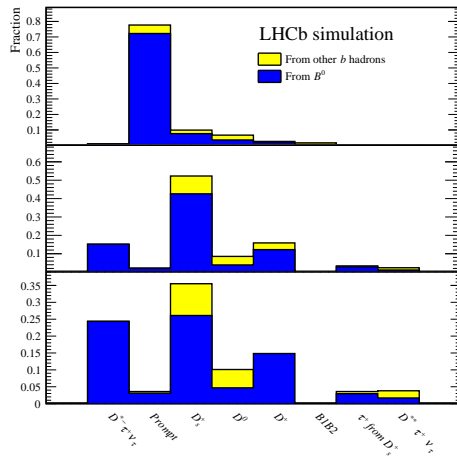
- Fit $m(D^{*\mp} 3\pi^\pm)$ for the number of B^0 candidates
 - Signal: sum of Gaussian and Crystal Ball with shared mean
 - Background: exponential function
- Fit $m(3\pi^\pm)$ in $5.20 < m(D^{*\mp} 3\pi^\pm) < 5.35$ GeV/ c^2 for number of D_s^+ candidates
 - Signal: Gaussian distribution
 - Background: exponential function
- N_{norm} is the difference of the two

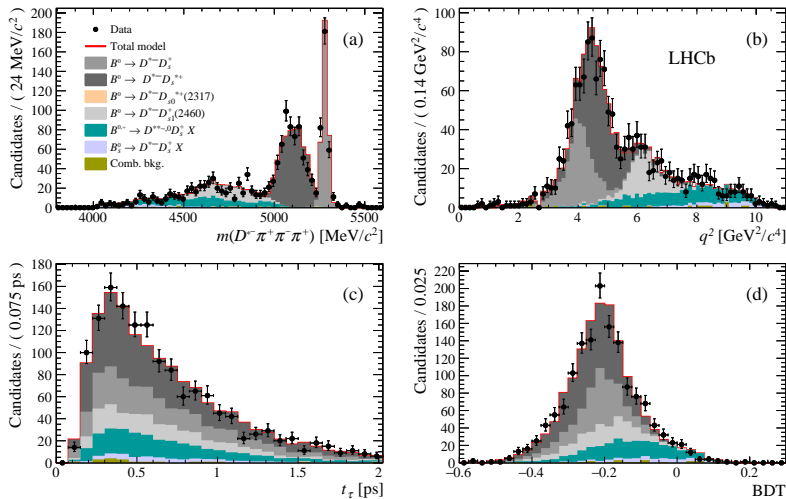
$$N_{\text{norm}} = 17660 \pm 143 (\text{stat}) \pm 64 (\text{syst}) \pm 22(D_s^+)$$

$R(D^*)$ hadronic: neutral isolation

$R(D^*)$ hadronic: $X_b \rightarrow D^{*\pm} 3\pi^\pm X$ MC sample

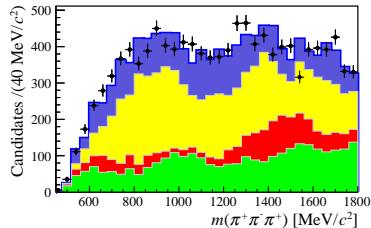
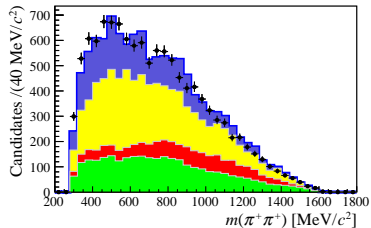
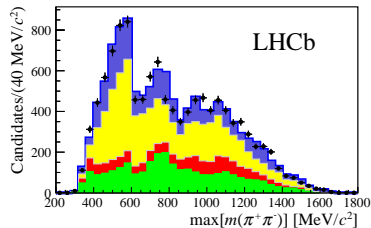
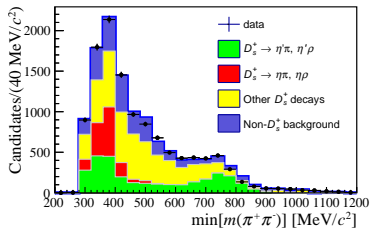
- Inclusive $X_b \rightarrow D^{*\pm} 3\pi^\pm X$ MC sample
- Shown: different parents of the $3\pi^\pm$ system
 - Blue: B^0
 - Yellow: other b -hadrons
 - Signal $B^0 \rightarrow D^{*-} \tau^+ \nu_\tau$
 - Prompt: directly from X_b
 - Charm (D_s^+, D^0, D^+)
 - $B1B2$: $3\pi^\pm$ and D^0 from different X_b
 - τ^+ from a D_s^+ decay
 - $D^{**} \tau^+ \nu_\tau$ (i.e. more highly-excited $D^{(*)}$ states)
- Top: after initial selection
- Middle: all candidates in the template fit
- Bottom: 3 highest BDT bins



$R(D^*)$ hadronic: $D^{*-}D_s^+$ control sample

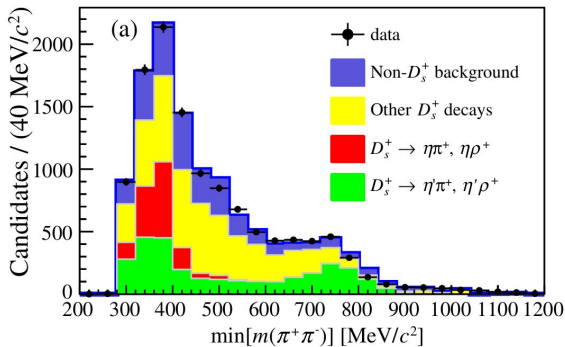
$R(D^*)$ hadronic: D_s^+ decay model

- $X_b \rightarrow D^{*-} D_s^+ X$ control sample obtained using BDT output



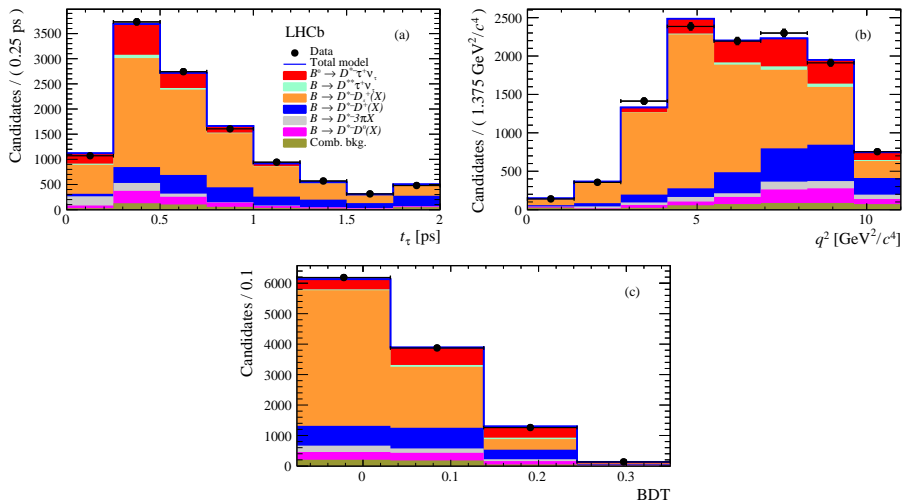
$R(D^*)$ hadronic: D_s^+ decay model

- $\tau^+ \rightarrow a_1(1260)^+(\rightarrow \rho^0\pi^+)\bar{\nu}_\tau$
- Dominant source of ρ^0 in D_s^+ decays due to $\eta' \rightarrow \rho^0\gamma$
- Crucial to describe η' contribution accurately
- Fit results used to describe the $D_s^+ \rightarrow 3\pi^\pm X$ model in the template fit



$R(D^*)$ hadronic: D_s^+ decay model fit results

D_s^+ decay	Relative contribution	Correction to MC
$\eta\pi^+(X)$	0.156 ± 0.010	
$\eta\rho^+$	0.109 ± 0.016	0.88 ± 0.13
$\eta\pi^+$	0.047 ± 0.014	0.75 ± 0.23
$\eta'\pi^+(X)$	0.317 ± 0.015	
$\eta'\rho^+$	0.179 ± 0.016	0.710 ± 0.063
$\eta'\pi^+$	0.138 ± 0.015	0.808 ± 0.088
$\phi\pi^+(X), \omega\pi^+(X)$	0.206 ± 0.02	
$\phi\rho^+, \omega\rho^+$	0.043 ± 0.022	0.28 ± 0.14
$\phi\pi^+, \omega\pi^+$	0.163 ± 0.021	1.588 ± 0.208
$\eta 3\pi$	0.104 ± 0.021	1.81 ± 0.36
$\eta' 3\pi$	0.0835 ± 0.0102	5.39 ± 0.66
$\omega 3\pi$	0.0415 ± 0.0122	5.19 ± 1.53
$K^0 3\pi$	0.0204 ± 0.0139	1.0 ± 0.7
$\phi 3\pi$	0.0141	0.97
$\tau^+(\rightarrow 3\pi(N)\bar{\nu}_\tau)\nu_\tau$	0.0135	0.97
$X_{nr} 3\pi$	0.038 ± 0.005	6.69 ± 0.94

$R(D^*)$ hadronic: fit projections

$R(D^*)$ hadronic: fit results

Fit component	Normalisation
$B^0 \rightarrow D^{*-} \tau^+ (\rightarrow 3\pi \bar{\nu}_\tau) \nu_\tau$	$N_{\text{sig}} \times f_{\tau \rightarrow 3\pi \nu}$
$B^0 \rightarrow D^{*-} \tau^+ (\rightarrow 3\pi \pi^0 \bar{\nu}_\tau) \nu_\tau$	$N_{\text{sig}} \times (1 - f_{\tau \rightarrow 3\pi \nu})$
$B \rightarrow D^{**} \tau^+ \nu_\tau$	$N_{\text{sig}} \times f_{D^{**} \tau \nu}$
$B \rightarrow D^{*-} D^+ X$	$f_{D^+} \times N_{D_s}$
$B \rightarrow D^{*-} D^0 X$ different vertices	$f_{D^0}^{V_1 V_2} \times N_{D^0}^{\text{sv}}$
$B \rightarrow D^{*-} D^0 X$ same vertex	$N_{D^0}^{\text{sv}}$
$B^0 \rightarrow D^{*-} D_s^+$	$N_{D_s} \times f_{D_s^+} / k$
$B^0 \rightarrow D^{*-} D_s^{*+}$	$N_{D_s} \times 1/k$
$B^0 \rightarrow D^{*-} D_{s0}^*(2317)^+$	$N_{D_s} \times f_{D_{s0}^*} / k$
$B^0 \rightarrow D^{*-} D_{s1}(2460)^+$	$N_{D_s} \times f_{D_{s1}^+} / k$
$B^{0,+} \rightarrow D^{**} D_s^+ X$	$N_{D_s} \times f_{D_s^+ X} / k$
$B_s^0 \rightarrow D^{*-} D_s^+ X$	$N_{D_s} \times f_{(D_s^+ X)_s} / k$
$B \rightarrow D^{*-} 3\pi X$	$N_{B \rightarrow D^* 3\pi X}$
B1B2 combinatorics	N_{B1B2}
Combinatoric D^{*-}	$N_{\text{not } D^*}$

$R(D^*)$ hadronic: fit results

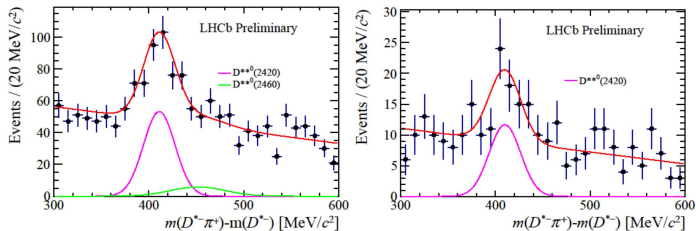
Parameter	Fit result	Constraint
N_{sig}	1296 ± 86	
$f_{\tau \rightarrow 3\pi\nu}$	0.78	0.78 (fixed)
$f_{D^{**}\tau\nu}$	0.11	0.11 (fixed)
$N_{D^0}^{\text{SV}}$	445 ± 22	445 ± 22
$f_{D^0}^{\text{V1V2}}$	0.41 ± 0.22	
N_{D_s}	6835 ± 166	
f_{D^+}	0.245 ± 0.020	
$N_{B \rightarrow D^* 3\pi X}$	424 ± 21	443 ± 22
$f_{D_s^+}$	0.494 ± 0.028	0.467 ± 0.032
$f_{D_{s0}^{*+}}$	$0^{+0.010}_{-0.000}$	$0^{+0.042}_{-0.000}$
$f_{D_{s1}^+}$	0.384 ± 0.044	0.444 ± 0.064
$f_{D_s^+ X}$	0.836 ± 0.077	0.647 ± 0.107
$f_{(D_s^+ X)_s}$	0.159 ± 0.034	0.138 ± 0.040
N_{B1B2}	197	197 (fixed)
$N_{\text{not}D^*}$	243	243 (fixed)

$R(D^*)$ hadronic: more detailed systematics

Contribution	Value in %
$\mathcal{B}(\tau^+ \rightarrow 3\pi\bar{\nu}_\tau)/\mathcal{B}(\tau^+ \rightarrow 3\pi(\pi^0)\bar{\nu}_\tau)$	0.7
Form factors (template shapes)	0.7
Form factors (efficiency)	1.0
τ polarisation effects	0.4
Other τ decays	1.0
$B \rightarrow D^{**}\tau^+\nu_\tau$	2.3
$B_s^0 \rightarrow D_s^{**}\tau^+\nu_\tau$ feed-down	1.5
$D_s^+ \rightarrow 3\pi X$ decay model	2.5
D_s^+ , D^0 and D^+ template shape	2.9
$B \rightarrow D^{*-}D_s^+(X)$ and $B \rightarrow D^{*-}D^0(X)$ decay model	2.6
$D^{*-}3\pi X$ from B decays	2.8
Combinatorial background (shape + normalisation)	0.7
Bias due to empty bins in templates	1.3
Size of simulation samples	4.1
Trigger acceptance	1.2
Trigger efficiency	1.0
Online selection	2.0
Offline selection	2.0
Charged-isolation algorithm	1.0
Particle identification	1.3
Normalisation channel	1.0
Signal efficiencies (size of simulation samples)	1.7
Normalisation channel efficiency (size of simulation samples)	1.6
Normalisation channel efficiency (modeling of $B^0 \rightarrow D^{*-}3\pi$)	2.0
Total uncertainty	9.1

$R(D^*)$ hadronic: feed-down systematics

- $B^0 \rightarrow D^{**}\tau\nu$ and $B^+ \rightarrow D^{**}\tau\nu$ constitute potential feed-down to the signal
- $D^{**}(2420)^0$ is reconstructed using its decay to $D^{*+}\pi^+$ **as a cross-check**
- The observation of the $D^{**}(2420)^0$ peak allows to compute the $D^{**}3\pi$ BDT distribution and to deduce a $D^{**}\tau\nu$ upper limit with the following assumption:
 - $D^{**0}\tau\nu = D^{**}(2420)^0\tau\nu$ (no sign of $D^{**}(2460)^0$)
 - $D^{**+}\tau\nu = D^{**0}\tau\nu$
- This upper limit is consistent with the theoretical prediction
- Subtraction in the signal of 0.11 ± 0.04 due to $D^{**}\tau\nu$ events leading to an error of 2.3%



$R(D^*)$ hadronic: prospects for systematics

Source	$\frac{\delta R(D^*)}{R(D^*)}$ [%]	Future
Simulated sample size	4.7	Produce more MC (fast simulation)
Empty bins in templates	1.3	
Signal decay model	1.8	
$D^{**}\tau\nu_\tau$ and $D_s^{**}\tau\nu_\tau$ feed-down	2.7	Measure $R(D^{**}(2420)^0)$
$D_s^+ \rightarrow 3\pi^\pm X$ decay model	2.5	BESIII measurement
$B \rightarrow D^* D_s^+ X$, $D^* D^+ X$, $D^* D^0 X$ backgrounds	3.9	Improves with stats
Combinatorial background	0.7	
$B \rightarrow D^{*-} 3\pi^\pm X$ background	2.8	Stronger rejection
Efficiency ratio	3.9	Improves with stats
Normalisation channel efficiency (modelling of $B^0 \rightarrow D^{*-} 3\pi^\pm$)	2.0	
Total systematic uncertainty	9.1	

$R(D^*)$ hadronic: prospects for systematics

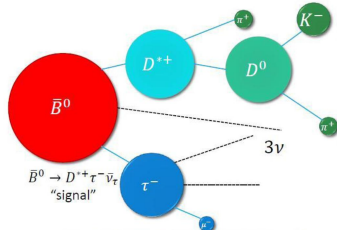
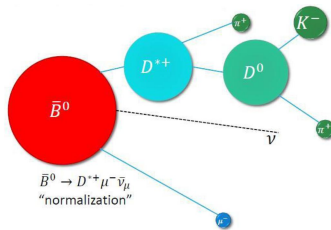
- Shape of $B \rightarrow D^*DX$ background (2.9%): scale with statistics
- $D_s^+ \rightarrow 3\pi X$ decay model (2.5%): BESIII future measurement.
- Branching fraction of $B^0 \rightarrow D^*3\pi$: can be precisely measured by Belle II.
- $B \rightarrow D^{*-}3\pi X$ background: strong cut on $\sigma_{\Delta z}$ between the τ and the D^0 vertices.
- With more data, measure $R(D^{**}(2420)^0)$ and constrain D^{**} feed-down
- Efficiency ratio: will improve with more data.

$$R(D^*) \text{ with } \tau^+ \rightarrow \mu^+ \nu_\mu \bar{\nu}_\tau$$

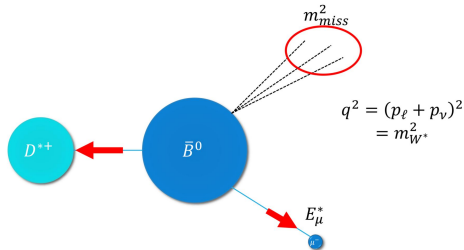
$R(D^*)$ muonic: kinematics

$$R(D^*) = \frac{\mathcal{B}(B^0 \rightarrow D^{*-} \tau^+ \nu_\tau)}{\mathcal{B}(B^0 \rightarrow D^{*-} \mu^+ \nu_\mu)}$$

with $\tau^+ \rightarrow \mu^+ \nu_\mu \bar{\nu}_\tau$



- Precise SM prediction: $R(D^*) = 0.258 \pm 0.005$ [HFLAV]
- Normalisation mode with the *same visible final state*
- $\mathcal{B}(\tau^+ \rightarrow \mu^+ \nu_\mu \bar{\nu}_\tau) = (17.39 \pm 0.04)\%$
- Separate τ and μ via a 3D binned template fit to:
 - $q^2 \equiv |P_{B^0} - P_{D^*}|^2$,
 - $m_{\text{miss}}^2 \equiv |P_{B^0} - P_{D^*} - P_{\mu^+}|^2$,
 - $E_{\mu^+}^* \equiv$ muon energy in B^0 rest frame.
- Background and signal shapes extracted from control samples and simulation validated against data



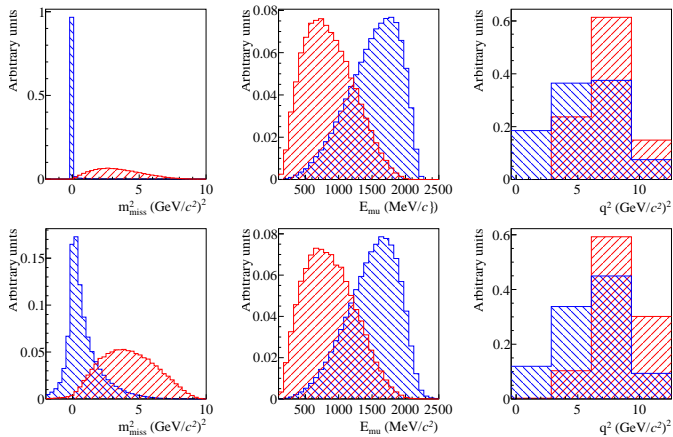
$R(D^*)$ muonic: kinematics

Problem of missing neutrino: no analytical solution for \vec{p}_B .

Approximate B momentum with $p_B^z = \frac{m_B}{m_{D^* \mu}} p_{D^* \mu}^z$ and exploit the measured B flight trajectory.

This leads to $\sim 18\%$ resolution on q^2 , m_{miss}^2 and E_μ^* , enough to preserve the discriminating features of the original variables.

$R(D^*)$ muonic: kinematics



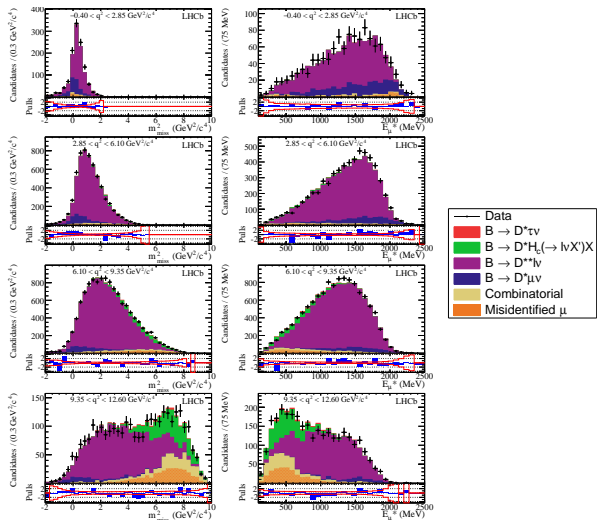
	$D^* \tau \nu_\tau$	$D^* \mu \nu_\mu$
m_{miss}^2	> 0	$\simeq 0$
E_μ^*	softer	harder
q^2	$> m_\tau^2$	> 0

τ mode (red) and μ mode (blue) using truth (top) and reconstructed (bottom) quantities.

$R(D^*)$ muonic: control samples

$\bar{B} \rightarrow [D_1, D_2^*, D_1'] \mu^- \bar{\nu}_\mu$ control sample.

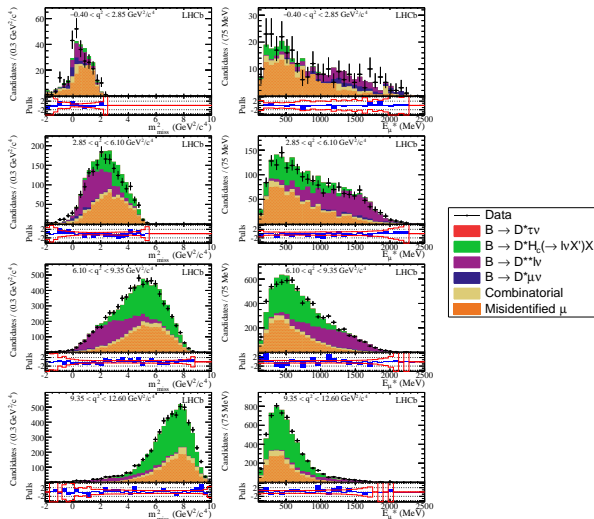
- Require exactly 1 track selected by the isolation MVA with the opposite charge to the D^{*+} candiadte.



$R(D^*)$ muonic: control samples

$\bar{B} \rightarrow D^{**}(\rightarrow D^{*+} \pi^+ \pi^-) \mu^- \bar{\nu}_\mu$ control sample.

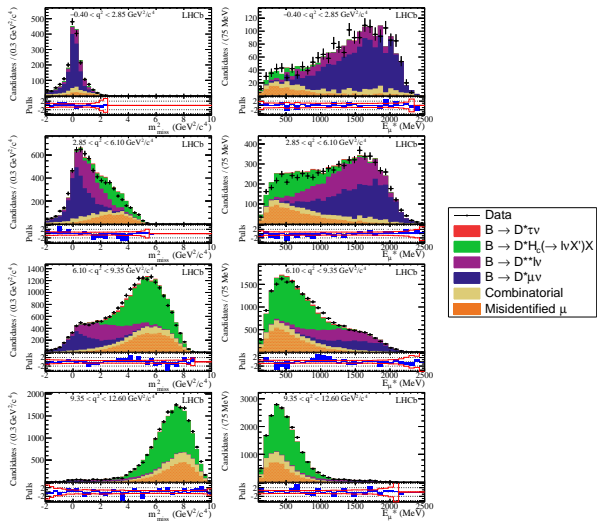
- Require exactly two tracks with opposite charge selected by the isolation MVA.



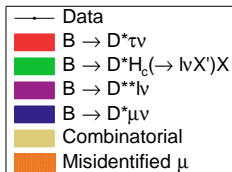
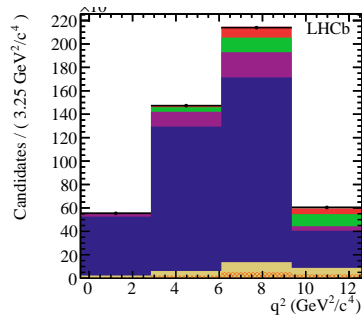
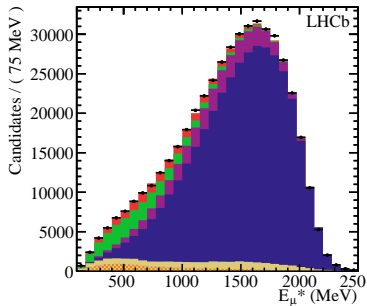
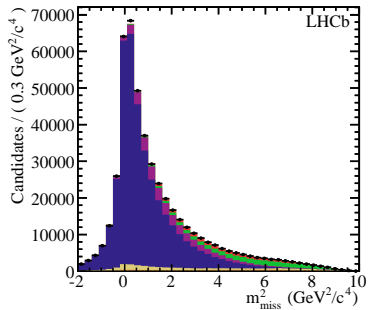
$R(D^*)$ muonic: control samples

$B \rightarrow D^{*+} X_c (\rightarrow \mu \nu X') X$ control sample.

- Require isolation MVA to identify a track consistent with the B vertex and at least one track with K^\pm hypothesis near the B .



$R(D^*)$ muonic: fit projections



$$R(J/\psi) \text{ with } \tau^+ \rightarrow \mu^+ \nu_\mu \bar{\nu}_\tau$$

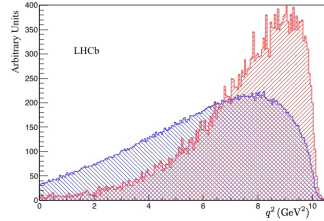
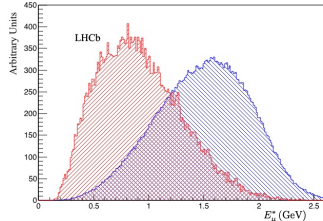
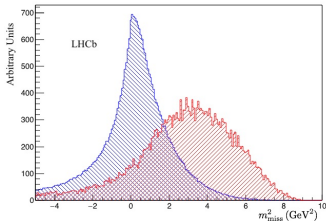
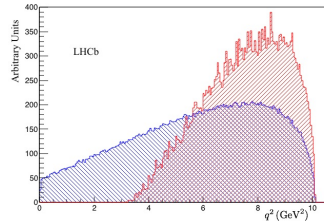
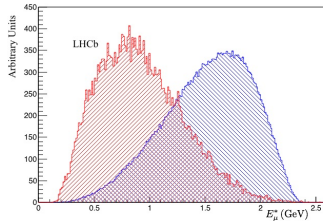
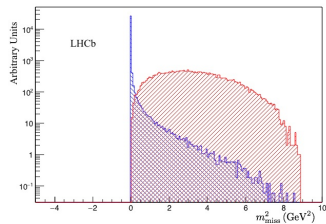
$R(J/\psi)$ muonic

- Generalisation of $R(D^*)$ to B_c^+

$$R(J/\psi) = \frac{\mathcal{B}(B_c^+ \rightarrow J/\psi \tau^+ \nu_\tau)}{\mathcal{B}(B_c^+ \rightarrow J/\psi \mu^+ \nu_\mu)}$$

- Prediction: $R(J/\psi) \in [0.25, 0.28]$ [PLB452 (1999) 120, arXiv:0211021, PRD73 (2006) 054024, PRD74 (2006) 074008]
- B_c^+ decay form factors not yet precise
- Like in $R(D^*)$, use m_{miss}^2 , E_μ^* and q^2 . Add information from B_c^+ decay time
- Imperfect reconstruction due to missing neutrinos. The broad shapes of the distributions are smeared but their discriminating power is preserved

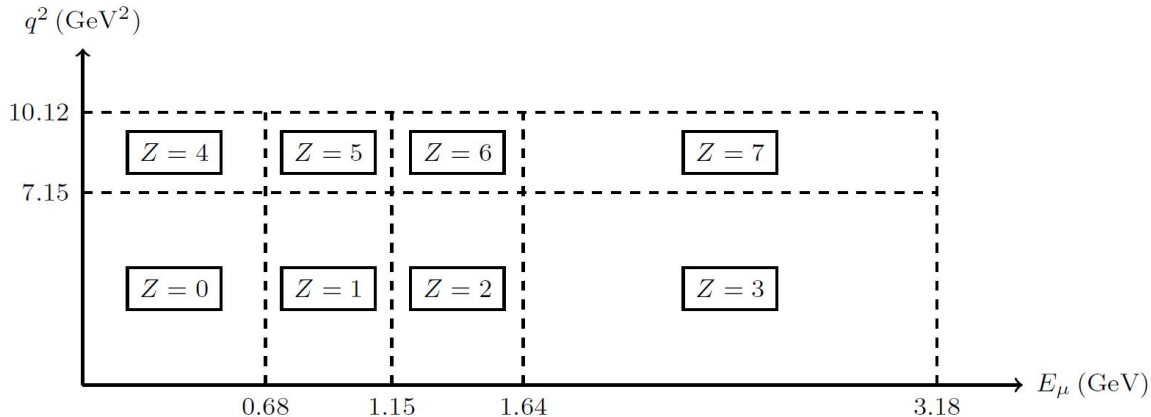
$R(J/\psi)$ muonic: kinematics



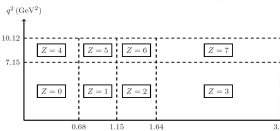
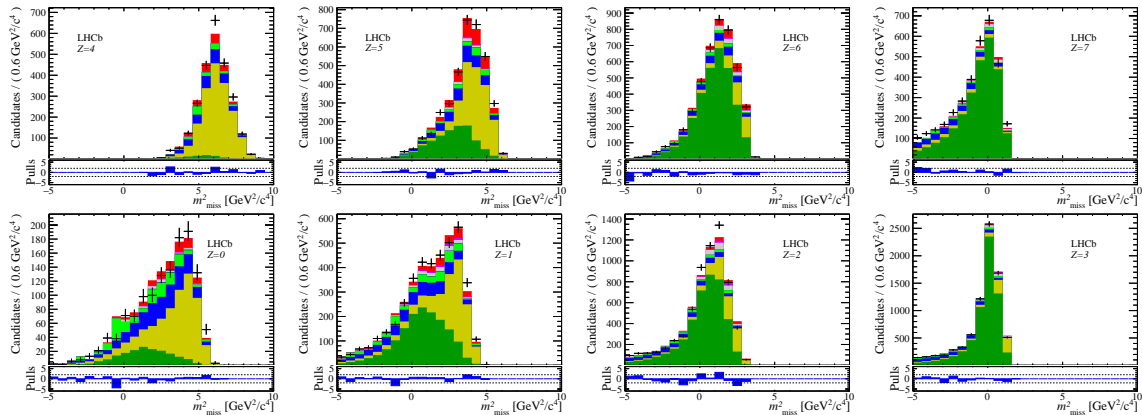
τ mode (red) and μ mode (blue) using truth (top) and reconstructed (bottom) quantities.

$R(J/\psi)$ muonic: Z variable

Trick to make a 3D fit with 4 variables: the Z variable merges information from q^2 and E_μ^*

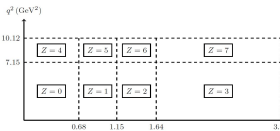
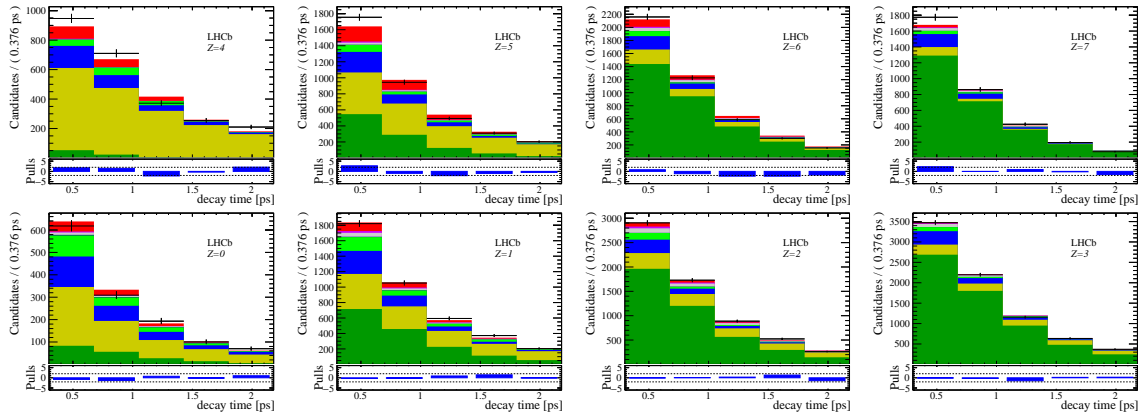


$R(J/\psi)$ muonic: fit projections in bins of Z



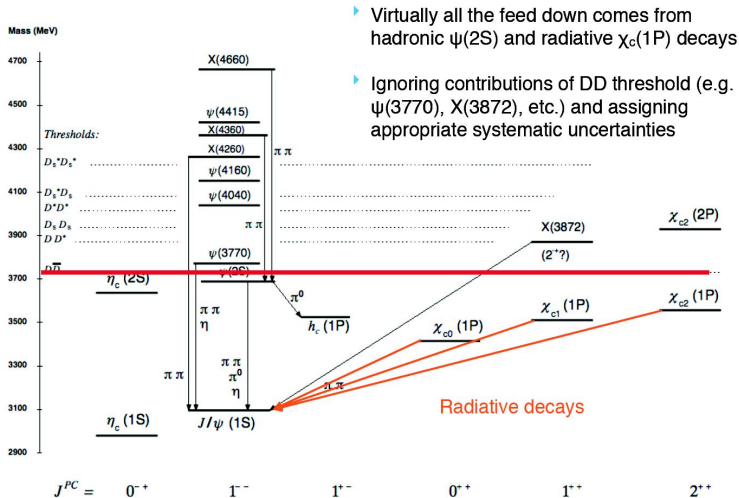
- \blackplus Data
- Mis-ID bkg.
- J/ψ comb. bkg.
- $B_c^+ \rightarrow \chi_c(IP)l^+ \nu_l$
- $B_c^+ \rightarrow J/\psi \tau^+ \nu_\tau$
- $B_c^+ \rightarrow J/\psi \mu^+ \nu_\mu$
- $J/\psi + \mu$ comb. bkg.
- $B_c^+ \rightarrow J/\psi H_c^+$
- $B_c^+ \rightarrow \psi(2S)l^+ \nu_l$

$R(J/\psi)$ muonic: fit projections in bins of Z



- $\text{---}+$ Data
- Mis-ID bkg.
- J/ψ comb. bkg.
- $B_c^+ \rightarrow \chi_c(IP)l^+ \nu_l$
- $B_c^+ \rightarrow J/\psi \tau^+ \nu_\tau$
- $J/\psi + \mu$ comb. bkg.
- $B_c^+ \rightarrow J/\psi H_c^+$
- $B_c^+ \rightarrow \psi(2S)l^+ \nu_l$

$R(J/\psi)$ muonic: feed-down



- ▶ Virtually all the feed down comes from hadronic $\psi(2S)$ and radiative $\chi_c(1P)$ decays
- ▶ Ignoring contributions of DD threshold (e.g. $\psi(3770)$, $X(3872)$, etc.) and assigning appropriate systematic uncertainties

Angular observables

Full angular distribution in $B \rightarrow D^*(\rightarrow D\pi)\ell\bar{\nu}_\ell$

The full angular distribution is given by

$$\frac{d^4\Gamma}{dq^2 d\cos\theta_\ell d\cos\theta_D d\chi} = \frac{3G_F^2 |V_{cb}|^2}{256(2\pi)^4 m_B^3} q^2 \left(1 - \frac{m_\ell^2}{q^2}\right)^2 \sqrt{\lambda_{D^*}(q^2)} \times B(D^* \rightarrow D\pi) \times \left\{ \right.$$

$$\begin{aligned} & [|H_+|^2 + |H_-|^2] \left(1 + \cos^2\theta_\ell + \frac{m_\ell^2}{q^2} \sin^2\theta_\ell\right) \sin^2\theta_D + 2[|H_+|^2 - |H_-|^2] \cos\theta_\ell \sin^2\theta_D \\ & + 4|H_0|^2 \left(\sin^2\theta_\ell + \frac{m_\ell^2}{q^2} \cos^2\theta_\ell\right) \cos^2\theta_D + 4|H_t|^2 \frac{m_\ell^2}{q^2} \cos^2\theta_D \\ & - 2\beta_\ell^2 \left(\Re[H_+ H_-^*] \cos 2\chi + \Im[H_+ H_-^*] \sin 2\chi\right) \sin^2\theta_\ell \sin^2\theta_D \\ & - \beta_\ell^2 \left(\Re[H_+ H_0^* + H_- H_0^*] \cos \chi + \Im[H_+ H_0^* - H_- H_0^*] \sin \chi\right) \sin 2\theta_\ell \sin 2\theta_D \\ & - 2\Re \left[H_+ H_0^* - H_- H_0^* - \frac{m_\ell^2}{q^2} (H_+ H_t^* + H_- H_t^*) \right] \cos \chi \sin \theta_\ell \sin 2\theta_D \\ & - 2\Im \left[H_+ H_0^* + H_- H_0^* - \frac{m_\ell^2}{q^2} (H_+ H_t^* - H_- H_t^*) \right] \sin \chi \sin \theta_\ell \sin 2\theta_D + 8\Re[H_0 H_t^*] \frac{m_\ell^2}{q^2} \cos\theta_\ell \cos^2\theta_D \left. \right\} \end{aligned}$$

$$\beta_\ell(q^2) = \sqrt{1 - \frac{m_\ell^2}{q^2}}$$

$$H(q^2) = \tilde{\varepsilon}^{\mu*} \langle D^*(\varepsilon) | J_\mu | \bar{B} \rangle$$

$B \rightarrow D^*(\rightarrow D\pi)\ell\bar{\nu}_\ell$: observables sensitive to NP

What can be extracted from the proposed observables:

$d\Gamma/dq^2$	$[H_+ ^2 + H_- ^2 + H_0 ^2] \left(1 + \frac{m_\ell^2}{2q^2}\right) + \frac{3}{2} \frac{m_\ell^2}{q^2} H_t ^2$	
$1 - \mathcal{A}_{\lambda_\ell}$	$ H_+ ^2 + H_- ^2 + H_0 ^2 + 3 H_t ^2$	
\mathcal{A}_{FB}	$ H_+ ^2 - H_- ^2 + 2 \frac{m_\ell^2}{q^2} \Re[H_0 H_t^*]$	
$R_{L,T}$	$ H_+ ^2 + H_- ^2$	
A_5	$ H_+ ^2 - H_- ^2$	
C_χ	$\Re[H_+ H_-^*]$	
S_χ	$\Im[H_+ H_-^*]$	(=0 in the SM)
A_8	$\Im\left[(H_+ + H_-)H_0^* - \frac{m_\ell^2}{q^2}(H_+ - H_-)H_t^*\right]$	(=0 in the SM)
A_9	$\Re\left[(H_+ - H_-)H_0^* - \frac{m_\ell^2}{q^2}(H_+ + H_-)H_t^*\right]$	
A_{10}	$\Im\left[(H_+ - H_-)H_0^*\right]$	(=0 in the SM)
A_{11}	$\Re\left[(H_+ + H_-)H_0^*\right]$	

Best discriminating variable to NP

$$\begin{aligned}
 \text{Heff} = & \frac{G_F}{\sqrt{2}} V_{cb} \left[(1 + g_V) \bar{c} \gamma_\mu b \right. \\
 & + (-1 + g_A) \bar{c} \gamma_\mu \gamma_5 b \\
 & + g_S i \partial_\mu (\bar{c} b) \\
 & + g_P i \partial_\mu (\bar{c} \gamma_5 b) \\
 & \left. + g_T i \partial_\nu (\bar{c} i \sigma_{\mu\nu} b) \right] (\bar{\ell} \gamma^\mu (1 - \gamma_5) \nu_\ell)
 \end{aligned}$$

×: “not sensitive”

***: “maximally sensitive”

Quantity	g_V	g_A	g_S	g_P	g_T
$\mathcal{A}_{\text{FB}}^D$	×	—	***	—	*
$\mathcal{A}_{\lambda_T}^D$	×	—	***	—	**
$\mathcal{A}_{\text{FB}}^{D*}$	*	***	—	***	*
$\mathcal{A}_{\lambda_T}^{D*}$	×	×	—	**	*
$R_{L,T}$	×	×	—	**	**
A_5	**	**	—	*	***
C_X	*	×	—	**	**
S_X	***	***	—	×	***
A_8	**	**	—	**	***
A_9	*	*	—	**	**
A_{10}	**	**	—	×	**
A_{11}	×	×	—	**	**